separations

MDPI

Article

Isolation and In Vitro Stability Studies of Edible Plant-Seed Derived (Raphani Semen) Nanoparticles

Jiahui An and Yi Zhu *

College of Food Science and Nutritional Engineering, China Agricultural University, 17 Qinghua Donglu, Beijing 100083, China

* Correspondence: zhuyi@cau.edu.cn; Tel.: +86-010-62737538

Abstract: (1) Background: Edible plant-derived nanoparticles contain large amounts of endogenous substances and can be used as carriers for disease treatment. However, the extraction rate and purity are not high. Raphani Semen, the dried seed of the *Raphanus sativus* L., has been used as food and medicine for clinical treatment and health care for many years. (2) Methods: This study began with the extraction of edible Raphani Semen-derived nanoparticles (ERDNs) by ultracentrifugation (UC). Then a new method was proposed for ERDNs to be extracted by polyethylene glycol (PEG) and purified by size exclusion chromatography (SEC), followed by SDS-PAGE for identified proteins. The stability of ERDNs was also verified in three digestion simulations. (3) Results: The PEG offered higher yields of 1.14–2.31 mg/g than UC. Transmission electron microscopy showed both UC and PEG with cup-shaped nanoparticles of around 200 nm. The SEC-purified ERDNs contained a range of proteins smaller than 70 kDa. The size stability of ERDNs in digestion solutions demonstrated their ability to withstand extreme conditions, confirming their potential as a nano drug delivery platform. (4) Conclusions: In conclusion, the data suggest that PEG+SEC could isolate ERDNs with high efficiency, providing a reference for the separation of other seed nanoparticles.

Keywords: edible nanoparticles; polyethylene glycol; size exclusion chromatography; Raphani Semen; seed

Citation: An, J.; Zhu, Y. Isolation and In Vitro Stability Studies of Edible Plant-Seed Derived (Raphani Semen) Nanoparticles. *Separations* **2023**, *10*, 218. https://doi.org/10.3390/separations10030218

Academic Editor: Gavino Sanna

Received: 17 February 2023
Revised: 15 March 2023
Accepted: 16 March 2023
Published: 21 March 2023

1. Introduction

Cruciferae plants (also known as Brassicaceae) are considered to be one of the most widely consumed plants in the world, due to their extensive cultivation area and huge family system (about 338 genera and 3709 species) [1]. The proportion of plant-based foods in the diet is positively associated with human health, as many studies have shown. The cruciferous are rich in nutrients such as amino acids, glucose, vitamin C, tocopherols, calcium, magnesium, and fiber, as well as many biologically active substances, including phenolic compounds, flavonoids, anthocyanins and carotenoids [2]. Unusually, the hydrolysis products (mainly isothiocyanates) of glucosinolates, a secondary metabolite unique to the cruciferous family, are thought to have potent anti-inflammatory and anti-cancer properties and may be used to treat hepatitis, diabetes, cardiovascular disease, inflammatory bowel disease (IBD), and to prevent obesity, menopausal syndrome, colon cancer, etc. [3,4]. In addition to cruciferous vegetables, consumption of other types such as rapeseed and mustard oils is widespread in Asia and Europe, ranging from about 3–5 kg per capita per year, up to 20 kg in some regions [5,6]. Raphani Semen is the seed of *Raphanus sativus* L., a traditional Chinese food herbal medicine that has long been used throughout the world to treat clinical indigestion, constipation, diarrhea, dysentery cough with phlegm, anemia, and menstrual disorders after stir frying or not [7,8]. More pharmacological effects are now being explored for their therapeutic effects on other diseases, including metabolic diseases, inflammatory, tumor, neurodegenerative diseases, and hypertension [9–13]. Raphani Semen contains more than 70 constituents, including isothiocyanates, organic acids, and

alkaloids, and stir frying increases the activity of isothiocyanates under appropriate conditions [14]. Although the health benefits of eating cruciferous vegetables are well known, the exact mechanisms and molecules by which they work are complicated, often involving a combination of components.

Exosomes are small extracellular vesicles (EVs) produced by living cells and enclosed in an outer phospholipid bilayer. Their structure was first discovered microscopically in plants but more definitive identification began with sheep reticulocytes [15,16]. Plant-derived extracellular vesicles (PDEVs) contain amino acids, nucleic acids, lipids, and bioactive substances that play an important role in the exchange of information between cells and organisms during growth [17]. Typically, animal exosomes are 30–150 nm in size, slightly smaller than PDEVs, and often contain cell membrane-specific marker proteins such as CD9, CD81, and CD63 as a result of secretion [18]. As exosomes are biologically derived, they often contain components specific from native cells. Animal exosomes have been used as general and cancer-specific surface-tethered molecules for early tumor monitoring [19]. Because of the protective properties of vesicle encapsulation around the contents, exosomes have been used to deliver drugs (including immunological modulators, therapeutic agents, and antisense oligonucleotides) to specific targets for the treatment of diseases [20]. However, disadvantages include low loading rates, poor stability, poor targeting, variable immunogenicity, and low economic viability. Plant-derived extracellular vesicles offer several advantages as a delivery platform. First, they have a higher extraction rate and could be produced economically on a larger scale. Second, they are highly stable during gastrointestinal digestion and in extreme environments. Finally, they could cross the blood-brain barrier and have lower biological toxicity and immunogenicity [21]. More importantly, the composition of PDEVs reflects the unique characteristics of each plant, which may also affect dietary health, such as different proteins, lipid profiles, and secondary metabolites, even miRNA. A variety of plant-derived exosome-like nanoparticles from lemon, mushroom, broccoli and grapefruit have antioxidant, anti-inflammatory, cross-talk modulating properties, and thermal and acid stability [22–25]. Zhang et al. found that rice-derived MIR168a could bind human/mouse LDLRAP1 mRNA and inhibit LDLRAP1 expression, thereby reducing LDL removal from mouse plasma [26]. This was the first evidence for the existence of cross-kingdom regulation of exogenous plant miRNAs, providing a possible mechanism by which plant exosome miRNAs may function. Ginger-derived exosome-like nanoparticles are taken up by intestinal macrophages without any negative effect on cell viability and they contain 6-gingerol, 6-shogaol, and mdo-miR7267-3p, which promotes mucosal tissue healing [22,27,28]. Thus, edible Raphani Semen-derived nanoparticles (ERDNs) may be a collection of beneficial substances such as carotenoids, miRNAs and proteins that enhance anti-inflammatory and anti-cancer effects from multiple angles. At the same time, the membrane structure facilitates the protection of beneficial components from being destroyed during digestion and thus reaching the site of disease.

To increase the possibility of their use, the development of simple, rapid, and accurate methods for the isolation of plant-derived exosome-like nanoparticles is a necessity. Despite the advantages of PDEVs in terms of drug delivery, active ingredients and economic benefits, there have been no specific standard methods for extraction, identification and evaluation as there are for animals [29]. Taking advantage of the similarities in size and morphology, the isolation of PDEVs was based on established methods of animal EVs. These included ultracentrifugation (UC using differential and density gradient), volume exclusion polymer (polyethylene glycol) precipitation, size exclusion chromatography (SEC), ultrafiltration membrane isolation, flow field flow fractionation (FFFF) and commercial kit. None of these methods, based on the size, morphology and density of the nanoparticles, was perfect. In fact, a combination of methods may be more appropriate. The most common method used to isolate EVs is ultracentrifugation, involving a series of centrifugations at progressively higher speeds to separate coarse debris, large cells and nanoparticles. To separate the different types of nanoparticles, they are usually purified by sucrose or OptiPrep gradient ultracentrifugation after a centrifugal force of 100,000$\times$ g to 150,000$\times$ g,

depending on the high g-force sedimentation and various gradient speeds [30,31]. However, repeated ultracentrifugation may lead to the destruction and aggregation of a large number of nanoparticles, which may affect downstream functional analysis and result in extremely low extraction rates [32]. In addition, an ultra-high-speed centrifuge is extremely expensive and can only be used for laboratory separations, so a more cost-effective polyethylene glycol (PEG) program is proposed. The polyethylene glycol program creates a net-like structure to precipitate the nanoparticles from the buffer and is often used to isolate large proteins and viruses [33,34]. Polyethylene glycol-isolated EVs are structurally similar to UC and have the potential to be economically produced on a large scale due to their ease of handling. However, the complexity of the plants tends to trap other impurities such as free proteins and pigments [35]. Further operations are usually required to improve their purity. Size exclusion chromatography is a multi-spaced stationary phase method for separating proteins and viruses according to molecular weight and size. Its innovative application to the separation of exosomes allows better preservation of structural integrity and biological activity due to its gravity-based guidance [36]. However, SEC takes longer to prepare and cannot be used in large batches. Therefore, it is usually used for the purification step in commercial kits (IZON qEV).

There are no studies that have confirmed the existence of Raphani Semen-derived nanoparticles. There is also no established method for extracting plant seeds derived nanoparticles due to the low water content and other characteristics. This study investigated (1) the possibility of ERDNs extraction; (2) whether animal EVs extraction methods, UC, PEG and SEC could be used to extract plant EVs; and (3) the stability of ERDNs in gastrointestinal digestion. This would provide the basis for further research into the pharmacology of Raphani Semen and the clinical applications of edible plant nanovesicle drug delivery platforms. In addition, this provided an opportunity for the development of functional food from Raphani Semen.

2. Materials and Methods

2.1. Differential Ultracentrifugation for the Isolation of ERDNs

The programs used to isolate the ERDNs were based on the cruciferous plant broccoli [24]. The pre-treatment of the samples was different. Raphani Semen (mantanghong, Chinese Academy of Agricultural Sciences, Beijing, China) was specially treated before centrifugation due to its granularity and viscosity. First, the Raphani Semen was soaked in water for 2 h to carefully remove the seed coat [37]. The peeled seeds were then ground to powder in the presence of liquid nitrogen. Finally, the powder was dissolved in PBS in a 1:1 (v/v) ratio and incubated at 37 °C for 30 min [38]. The supernatant was collected separately after the differential centrifugation sequence at 1000× g for 10 min, 3000× g for 20 min and 10,000× g for 40 min. After the last centrifugation step, the supernatant was passed through a 0.22 μm filter membrane and then centrifuged for 90 min at 150,000× g with a type 70Ti rotor (Beckman Coulter, Brea, CA, USA). After this step, the sediment nanoparticles were collected and resuspended in PBS. Another centrifugation at 150,000× g for 90 min was performed to further purify the ERDNs. All centrifugation steps were performed at 4 °C to ensure the integrity of the nanoparticles. The final nanoparticles were resuspended in PBS (pH = 7) and the protein concentration of the ERDNs was measured using a BCA assay kit (Solarbio, China). Samples were stored at 4 °C for subsequent measurements. All samples should be stored for a maximum of one week to ensure a complete assay.

2.2. Polyethylene Glycol Solution for Precipitation ERDNs

Nanoparticles can be purified by virus isolation methods because they are similar in size and physiological properties. Polyethylene glycol of different molecular weights (Mn) had been used to isolate the virus and protein [39,40]. In this study, PEG 8000 (89510, Sigma-Aldrich, St. Louis, MO, USA) was prepared as a 40% (w/v) stock solution with ultrapure water after sonication for 30 min and passed through a 0.22 μm filter membrane to remove impurities. The PEG 8000 precipitation was identical to the UC method in

the differential centrifugation steps. Unusually, after centrifugation at 10,000× *g*, the supernatant was passed through 0.22 μm membrane filtration. Then an equal volume of supernatant was mixed with PEG 8000 solution to a final concentration of 5%, 8%, 10%, 12%, 15% and 20% (*w*/*v*). The mixtures were incubated overnight at 4 °C for over 12 h. The PEG 8000 solution was thoroughly mixed with the supernatant, centrifuged at 4 °C for 30 min at 8000× *g* and again passed through a 0.22 μm filter membrane. The centrifuge tube was inverted for 5–10 min to completely remove the supernatant, and the precipitate was resuspended with 1 mL of PBS by shaking for 10 min. To improve the precipitation rate of ERDNs, sonication was used instead of incubation for 30 min in the pre-treatment phase. In addition, a final concentration of 100 mM sodium chloride (NaCl) was added during the overnight precipitation phase. The proteins of the samples were quantified using the BCA assay kit and stored at 4 °C for subsequent analysis.

2.3. Physical and Chemical Characterization of ERDNs

The nanoparticles obtained required further size and morphology measurements to determine their authenticity and stability. The size distribution of the ERDNs was measured by dynamic light scattering (DLS), which is related to the intensity of the light scattered by the particles, using the Zetasizer nano 3000 (Malvern, Southborough, MA, USA). The ERDNs were subjected to three consecutive hydrodynamic size measurements at 25 °C. In the experiment, the refractive index (RI) of PBS was chosen to be 1.338. The RI and absorption of ERDNs were set at 1.38 and 0.01, respectively, according to the previous protocol [41]. The reported values were the combined results of at least three different batches of samples and were analyzed using Zetasizer software (Malvern). The morphology of the ERDNs was observed using JEM 1200EX (JEOL Ltd., Akishima, Japan). The samples were negatively stained with 1% uranium acetate and dried at room temperature prior to imaging. Before physical characterization, all samples were diluted with PBS to the appropriate concentration and passed through a 0.22 μm filter membrane. PBS, PEG8000, NaCl and other solutions were all passed through the particle size measurement after preparation to ensure no new particles were introduced.

The elemental composition of the ERDNs surface was measured by X-ray Photoelectron Spectroscopy (XPS) using ESCALAB 250Xi (Thermo Scientific, Waltham, MA, USA). Freshly prepared ERDNs were dissolved in PBS and filtered through a 0.22 μm membrane. It was dropped onto a silicon wafer and dried at room temperature, and then it was vacuumed into the XPS test system. The sample was excited using Al Kα radiation at 1486.2 eV as a probe. The high-resolution spectra were measured at a flux energy of 20.0 eV, using an energy step of 0.1 eV. The main C1s peak of the carbon atom was used as a reference for all spectra with a value of 284.8 eV. Data were pooled in Thermo Avantage 5.992 software for analysis.

2.4. Stability of ERDNs In Vitro Simulated Digestion

The stability of the ERDNs was evaluated using the standard static in vitro digestion method applicable to food [42]. Briefly, salivary α-amylase (A0521, Sigma, Sigma-Aldrich, St. Louis, MO, USA), porcine pepsin (P7000, Sigma, Sigma-Aldrich, St. Louis, MO, USA), bile salts (G8310, Solarbio, Beijing, China) and pancreatin (P7545, Sigma, Sigma-Aldrich, St. Louis, MO, USA) were added to the simulated electrolyte stock solution to prepare simulated salivary fluid (SSF), simulated gastric fluid (SGF) and simulated intestinal fluid (SIF). All three digestion solutions were prepared at 1.25× concentration. The component digestion stock solutions were dispersed in distilled water into 80 mL to give a final volume of 100 mL of electrolyte stock solution. After adjustment to the appropriate pH, the electrolyte stock solutions, except for the $CaCl_2(H_2O_2)_2$, were stored at −20 °C. This is because precipitation may occur with the addition of $CaCl_2(H_2O_2)_2$. The enzymes, bile salts and $CaCl_2(H_2O_2)_2$ were dissolved in the electrolyte stock solutions to prepare them for use. The $CaCl_2(H_2O_2)_2$ was dissolved in water. The sum of the volume of water and calcium ion solution was a quarter of the electrolyte stock solution. Table 1 shows the

amount of each component to be added when the final digestion solution is 50 mL. At each step, the ERDNs were added to the simulated digestion solution in the same volume (50:50, *v*/*v*) and incubated at 37 °C at 200 rpm. The pH of the digestion system was corrected at any time during the experiment. The ERDNs were incubated in SSF for 2 min for particle size measurements. At the same time, they were incubated in SGF and SIF for 2 h and were taken out every 30 min to measure particle size. Two successive digestion steps were performed. First, ERDNs were incubated in SSF for 2 min and then were incubated in SGF and SIF for 2 h. Secondly, ERDNs were incubated in SGF for 2 h and then in SIF for 2 h. In this process, half of the solution of the previous digestion stage was taken out and mixed with the digestion solution of the next stage in equal volume. All reagents required pre-warming at 37 °C. All digestion samples were diluted with PBS and passed through a 0.22 μm filter membrane prior to measurement.

Table 1. Preparation of simulated digestion stock solution. Simulated salivary fluid (SSF, pH = 7, 2 min), simulated gastric fluid (SGF, pH = 3, 2 h) and simulated intestinal fluid (SIF, pH = 7, 2 h) were prepared at 1.25× concentration.

			SSF(pH = 7)		SGF(pH = 3)		SIF(pH = 7)	
Constituent	**Stock Solution**		**Volume**	**Concentration**	**Volume**	**Concentration**	**Volume**	**Concentration**
	g/500 mL	**mol/L**	**mL**	**mmol/L**	**mL**	**mmol/L**	**mL**	**mmol/L**
KCl	18.5	0.5	3.02	15.1	1.38	6.9	1.36	6.8
KH_2PO_4	34	0.5	0.74	3.7	0.18	0.9	0.16	0.8
$NaHCO_3$	42	1	1.37	13.7	2.55	25.5	8.5	85
NaCl	58.5	2			2.36	47.2	1.92	38.4
$MgCl_2(H_2O)_6$	15.25	0.15	0.1	0.15	0.08	0.1	0.22	0.33
NH_4Cl	26.75	1	0.012	0.12	0.1	1		
Add H_2O_2 to			80		80		80	
Composition of the final solution								
Electrolyte stock solution			40		40		40	
$CaCl_2(H_2O_2)_2$	44.1	0.3	0.25	1.5	0.025	0.15	0.2	0.6
α-amylase			0.0025 g	150 U/mL				
Pepsin					0.8 g	4000 U/mL		
Pancreatin							0.05 g	200 U/mL
Bile							0.629 g	20 mM
Add H_2O_2 to			50		50		50	

2.5. Purification of ERDNs by Size Exclusion Chromatography

Size exclusion chromatography has traditionally been used to separate proteins of different molecular weights and to purify EVs in body fluids [43,44]. In this study, Sephacryl S-500 (Biotop, Beijing, China) was balanced at room temperature and cleaned with ultrapure water to remove the ethanol protective solution. Sephacryl S-500 (Sephacryl S-500: ultrapure water = 5:1, *v*/*v*) was then slowly introduced into the chromatographic column (φ16 mm, 20 cm) using a glass rod, taking care not to form bubbles. The chromatographic column was filled under gravity with 16 cm of Sephacryl S-500 for 2 h. After complete precipitation of the Sephacryl S-500, the column was equilibrated with at least three times the bed volume of ultrapure water and five times the bed volume of PBS (pH = 7). After passing through a 0.22 μm filter membrane, 0.5 mL of ERDNs was added to the top of the column and allowed to flow under gravity. When the liquid began to drop slowly, 0.5 mL of PBS buffer solution (pH = 7) was added to the top volume. Finally, a total of 25 consecutive fractions with 0.5 mL were collected in a centrifuge tube at the bottom. After use, the chromatographic column was cleaned with at least five times the bed volume of PBS (pH = 7). The protein concentration was determined by measuring the absorbance at 280 nm using Nano-300 (Jiapeng, Shanghai, China). The particle sizes of all 25 fractions were properly diluted and measured by DLS.

2.6. SDS-PAGE Analysis of ERDNs

To further determine the protein composition of ERDNs. The 25 fractions purified by SEC were mixed with a 5× SDS-PAGE loading buffer (Solarbio, Beijing, China) and boiled at 100 °C for 5 min to denature the protein. In total, 10 µL of the fractions were loaded onto a 5% polyacrylamide concentrated gel and the 10% polyacrylamide separated gel in 1× running buffer (25 mM Tris, 192 mM glycine and 0.1% SDS, pH 8.3) and then electrophoresed at 80 V for 30 min and 120 V until bromophenol blue migrated to the bottom. After electrophoresis, the concentrated gel was carefully removed and the separated gel was immersed in Coomassie Brilliant Blue ultrafast dye solution (Beyotime, Shanghai, China) and shaken slowly for 30 min to guide the development of visible bands. Finally, the gels were washed with ultrapure water for 8 h and photographed for documentation.

2.7. Statistical Analysis

All data were analyzed using SPSS software (IBM SPSS Statistics 19) and expressed as mean and SEM unless otherwise stated. Figures were generated using Origin software (Origin 2022b). Shapiro-Wilk and Kruskal-Wallis tests were used to test whether the data were normally distributed. A two-sample t-test was used to compare the means of two groups. One-way ANOVA was used to evaluate three or more experimental groups with LSD and Games-Howell tests for significance level. The results presented were the mean of at least three independent experiments. The *p*-value less than * 0.05 was considered statistically different.

3. Results and Discussion

3.1. ERDNs Isolated by Ultracentrifugation

In this study, the nanoparticles extracted from the seeds of the *Raphanus sativus* L., Raphani Semen were successfully used. The results showed that ERDNs particles were obtained after UC with a yield of 0.17 ± 0.017 mg/g and the mean size of the ERDNs was 193.4 ± 8.60 nm with a peak diameter of 164.2 nm from DLS (Figure 1). The morphology and size of the particles were observed using transmission electron microscopy (TEM) in Figure 1, which shows that the ERDNs were wrapped in a phospholipid bilayer membrane with a typical cup-like appearance. The size of the electron microscopy results was around 200 nm.

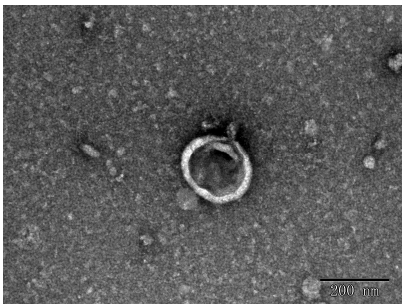

(**a**)

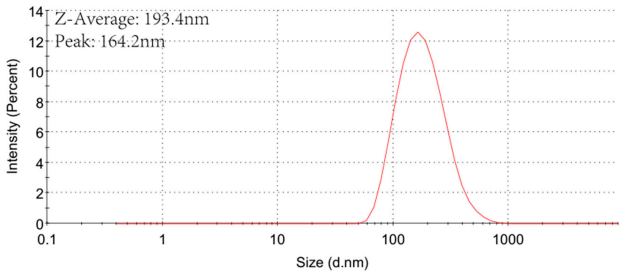

(**b**)

Figure 1. Characterization of ERDNs separated by UC: (**a**) Transmission electron microscopy (TEM) characterization of edible Raphani Semen-derived nanoparticles (ERDNs). (**b**) The mean particle size of ERDNs was measured by dynamic light scattering (DLS). All samples were diluted to the appropriate concentration with PBS.

Ultracentrifugation is considered the gold standard for conventional exosome isolation and has been used in most studies of animal or plant EVs. Due to the complex diversity of proteins, miRNAs, lipids and bioactive substances of PDEVs, there is no uniform and established method for their identification [45], although plant and animal EVs have shown similarities in protein composition. To distinguish their differences in biogenesis, most plant EVs are referred to PDEVs or plant-derived exosome-like nanoparticles (PELNs) [22,46–48].

The ERDNs were isolated with reference to several previous studies [24,37,38,49]. Due to the low water content, Raphani Semen cannot be directly juiced like grapes and ginger. At the same time, in order to avoid impurities introduced by the skin, the seed coat of the Raphani Semen was removed by soaking it in water for 2 h. Then the peeled Raphani Semen was completely dissolved and dispersed in PBS at 37 °C for 30 min after sufficient grinding at low temperatures. For low-speed centrifugation, large particles of contaminants, fibers and cell debris were removed after centrifugation at 1000× *g*, 3000× *g* and 10,000× *g*, respectively. Depending on the general diameter range of PDEVs' 30–200 nm, the supernatant collected after low-speed centrifugation was passed through a 0.22 μm filter membrane to remove large molecules such as free protein aggresomes from the fragmented cells to improve the extraction rate of ERDNs [33].

The yields in this study are slightly lower than in previous studies. Plants usually secrete high levels of nanovesicles, for example, 1.76 mg/g in grapes, 2.21 mg/g in grapefruit and 0.44 mg/g in tomato [50]. This may be because mature plants have more intercellular communication. The size of PDEVs tends to vary. Wang et al. isolated grapefruit-derived nanovesicles with 210.8 ± 48.62 nm [49]. In another study, the average diameter of nanovesicles isolated from broccoli was only 32.4 nm [24]. Vesicles extracted from ginger were purified to yield two populations of different sizes (about 294 nm and 386 nm), with a peak average size of approximately 400 nm [33]. The size of ERDNs in this study was around 200 nm, which was within the normal range of most EVs. The slightly smaller size observed by TEM compared to DLS may be due to the different test environments. The DLS measured the hydrodynamic diameter while TEM measured it in a dehydrated state [51].

3.2. PEG8000 Can Be Used for the Enrichment of ERDNs

As shown in Figure 2, when PEG 8000 was used, the yield of ERDNs was 1.14–2.31 mg/g, significantly higher than the UC method (even at 5%). The yield of ERDNs was lowest at 5%, and when the concentration was increased further, the yield was slightly but not significantly higher($p > 0.05$). Generally speaking, the incubation time was proportional to the production [52]. The incubation time of this study was more than 12 h. When the concentration of PEG 8000 was increased from 5% to 8%, the concentration of ERDNs increased significantly, suggesting that there may be a critical micelle-like concentration between them [53]. The PEG 8000 precipitation results were slightly higher than those for ginger edible nanoparticles (an efficiency of 60–90% for PEG6000 compared to UC) [33]. To further improve the yield of ERDNs, 37 °C incubation was replaced by sonication during pre-treatment (5 s intervals for every 10 s of work for 30 min). The high oil content of the Raphani Semen itself reduced the solubility in the PBS buffer. Sonication significantly improved the homogeneity of the system compared to incubation. The results in Figure 2 also showed that the yield of ERDNs was significantly higher in the sonication group than in the incubation group for PEG8000 of 5% and 8% ($p < 0.05$). In combination with NaCl, PEG was used for virus precipitation or secondary concentration [54]. Whether the ionic strength during PEG8000 incubation could improve ERDNs extraction was also studied. In this study, the addition of 100 mM NaCl did not increase the yield of ERDNs in most cases. However, in operation, it did increase the clarity of the PEG8000 after overnight incubation. Sonication and NaCl did not change the particle size of PEG 8000 at low concentrations (8%, 10% and 12%), but increased it at 15% and 20%. Therefore, NaCl will not be used for future research. The peak particle size of ERDNs also remained stable under a low concentration of PEG 8000(Figure 2).

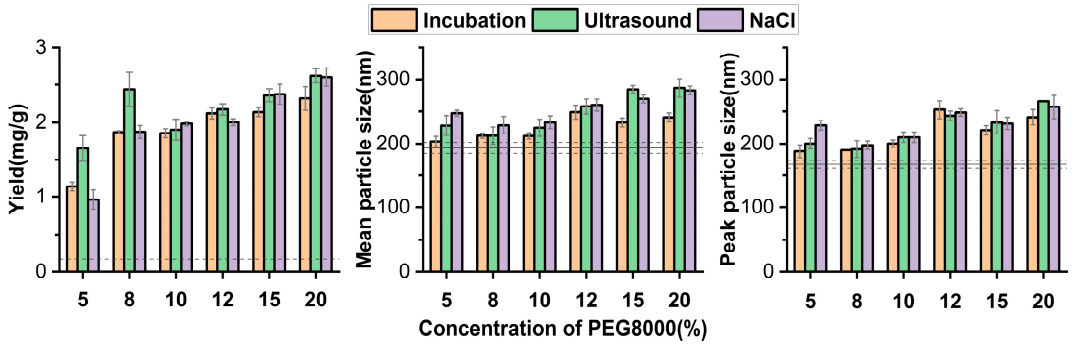

Figure 2. The ERDNs were precipitated by PEG8000: The yield, mean particle size and peak particle size of ERDNs extracted by PEG8000 with different concentrations (%, w/v). The mass of ERDNs was calculated by protein and the mass of Raphani Semen was calculated by powder. The dotted line in the graph shows the yield, mean particle size and peak particle size of ERDNs extracted by ultracentrifugation.

Figure 3 shows a TEM image of 8% PEG8000 extracted ERDNs. The results of this study also confirm the possibility that PEG could be used to extract EVs. Plants often contain large molecules such as starch, cellulose and tannins, which increase viscosity and make centrifugation difficult [55]. Thus, PEG is used as a lubricant for medical devices and a food additive [56]. Polyethylene glycol solutions have been used to concentrate and purify viruses for more than 50 years [57]. Viruses are thought to emerge from exosomes and vice versa and the hydrophobic nature of the lipid bilayer makes the use of PEG to precipitate exosomes a cost-effective method [58,59].

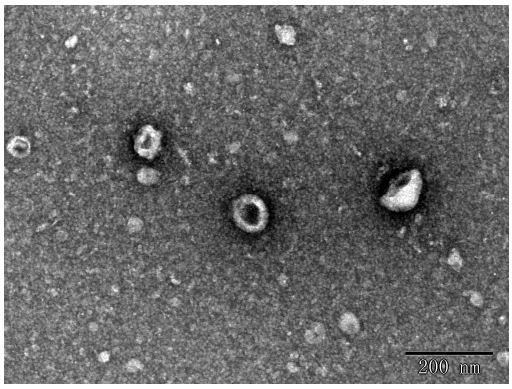

Figure 3. TEM characterization of ERDNs precipitated by PEG8000.

Previous studies have shown that the mean size of recovered exosomes is the same at each concentration of PEG, and that the mode particle size is negatively correlated with PEG concentration [58]. Surprisingly, the mean particle size of the ERDNs increased at higher concentrations (12%, 15% and 20%) and was larger than the ERDNs of UC (Figure 2). This may be because the residual PEG 8000 in the precipitate affected the measurement of the hydrodynamic diameter. In addition, the precipitation of other impurities (pigments, phenols and flavonoids) could bind to the ERDNs during the overnight incubation [53]. To obtain ERDNs similar to UC, further purification of the PEG8000-precipitated ERDNs was necessary. In some studies, residual PEG may interfere with certain analyses that require high-purity products such as mass spectrometry. Size exclusion column chromatography, dialysis, SDS-PAGE, cesium chloride and potassium chloride precipitation methods were used to eliminate these effects [60–62].

3.3. Sephacryl S-500 Column for Purification of ERDNs

The acceptable daily intake (ADI) of polyethylene glycol (E1521, molecular weight 300–10,000) for use as a food additive was established by JECFA at 10 mg/kg bw per day in case of possible overestimation [52]. The final residual PEG content of the nanoparticles inevitably increased with the concentration of PEG added during the incubation and the use of higher concentrations of PEG (12% and 15%) significantly inhibited the contents (total polyphenols, antioxidant capacity and RNA) [33]. In addition, the viscosity of the system gradually increased with increasing PEG8000 concentration, which was detrimental to the subsequent dispersion of the ERDNs-precipitated aggregates. Therefore, in line with previous studies (8%, 10% and 12%) PEG8000 had a significantly increased yield and the particle size distribution of 8% PEG 8000 was relatively stable; the 8% was used in follow-up experiments.

In this work, the Sephacryl S-500 stationary phase was used for the purification of ERDNs from an 8% PEG 8000 precipitation. As shown in Figure 4, the proteins started to appear in fraction 14 and the ERDNs in fraction 15. The PEG-precipitated ERDNs were passed through the SEC column at room temperature for approximately 50 min. The ERDNs of different particle sizes were present between fractions 15–24, with the larger particles appearing before the smaller ones. The result of this macromolecule flowing out first and small molecule flowing out later conformed to the manufacturer's instructions. It allowed rapid and reproducible purification of proteins, polysaccharides and other macromolecules on a laboratory and industrial scale [63]. You JY et al. found that SEC gave higher purity and extraction rates compared to UC and PEG precipitation [36].

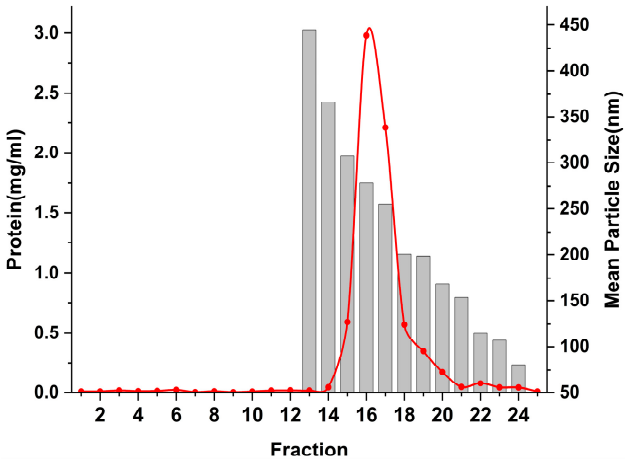

Figure 4. The protein content and mean particle size of each component after separation by SEC. The protein content was calculated by the absorbance value at 280 nm.

An SDS-PAGE analysis of all the fractions showed significant protein bands in fractions 15 to 18, with molecular weights concentrated in the 70 kDa range (Figure 5). The molecular weight of exosomal proteins found in human cerebrospinal fluid was also concentrated in the range of 70 kDa [43]. Zu et al. showed that the nanoparticles of tea leaves contained a population of proteins with a molecular weight of between 10 and 15 kDa [51]. Meanwhile, exosome-like nanoparticles from ginger and oat contain a protein composition similar to that of the tissue [28,57]. The expected molecular weight of the protein was observed in the vesicular fractions of sunflower apoplastic fluids and compared with sunflower lectin and FSGTP1 [37]. As in these results, the low molecular weight protein bands may also contain markers for PDEVs.

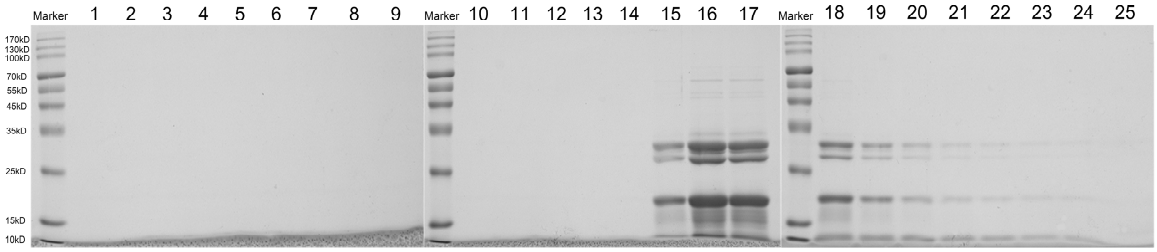

Figure 5. SDS-PAGE shows that proteins with different molecular weights appeared in the 15–24 fraction in the same volume.

The surface element content and composition of the ERDNs extracted by the three methods were measured by XPS. Figure 6 and Table 2 showed that UC, PEG and PEG+SEC all exhibited characteristic signals corresponding to C1s, N1s and O1s. The high content of N elements in PEG may indicate interference from free proteins. Purification by SEC reduced the N content and increased the C and O content. High-resolution mapping showed that the ERDNs extracted by all three methods had peaks corresponding to C-C, C-O-C, O-C=O, C=O and C-O, which may correspond to aliphatic and aromatic Cs such as flavonoids and polyphenols [64]. The peaks corresponding to C-NH_2 may include amino acids and peptide backbone [65].

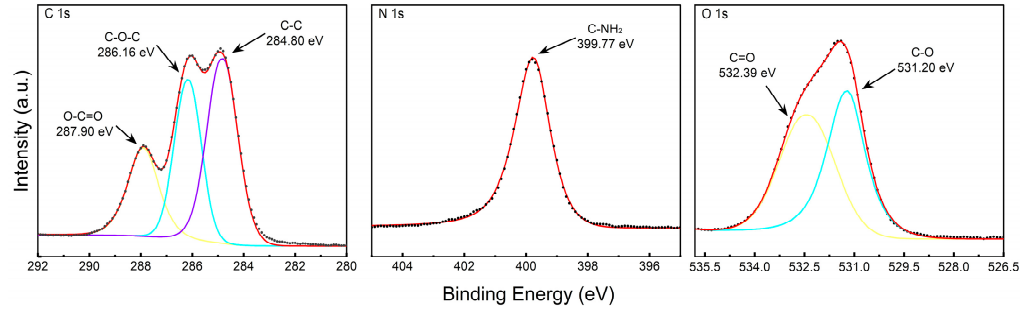

(**a**)

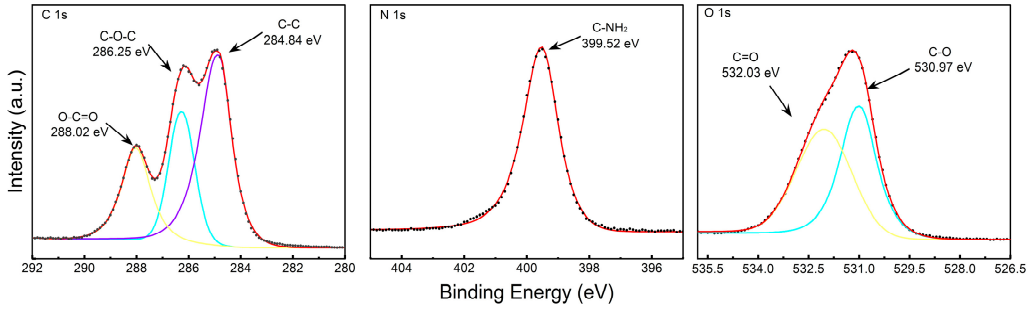

(**b**)

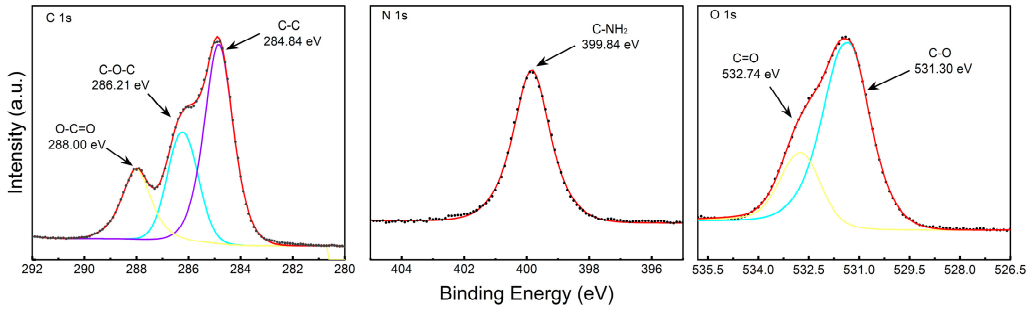

(**c**)

Figure 6. *Cont.*

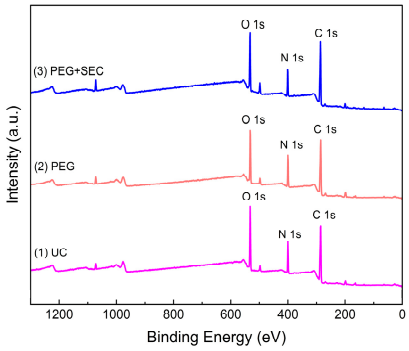

(**d**)

Figure 6. X-ray Photoelectron Spectroscopy (XPS) of UC, PEG, PEG+SEC methods of ERDNs extraction: High-resolution spectra of C 1 s, N 1 s and O 1 s obtained by (**a**) UC, (**b**) 8% PEG8000 and (**c**) PEG+SEC. (**d**) Full spectrum scan results.

Table 2. Elemental content of ERDNs obtained by the UC, PEG, and PEG+SEC measured by XPS.

UC	Binding Energy(eV)	Atomic%
C1s	285.27	64.67
N1s	399.72	13.84
O1s	531.53	21.49
PEG	Binding Energy (eV)	Atomic%
C 1s	284.85	64.79
N 1s	399.56	15.4
O 1s	531.3	19.81
PEG+SEC	Binding Energy (eV)	Atomic%
C 1s	284.8	67.26
N 1s	399.63	12.42
O 1s	531.29	20.32

3.4. Stability of ERDNs in Simulated Gastrointestinal Digestion

Stability studies were performed by sequentially exposing the ERDNs to SSF (pH = 7, 2 min), SGF (pH = 3, 2 h) and SIF (pH = 7, 2 h). The particle size of the ERDNs represents the stability in the simulated digestion process in Figure 7. As shown in previous studies, the particle size and extraction rate of exosomes may be related to the pH of the solution [66,67]. In this study, the size of the ERDNs did not change significantly during the 2 h of gastric digestion, 2 h of intestinal digestion and 2 min of oral digestion ($p > 0.05$). This suggests that ERDNs are stable in extreme environments and help to protect the miRNAs, proteins and bioactive compounds they contain from damage. Furthermore, the ability of PDEVs to withstand mechanical and enzymatic adversity has been shown to provide new evidence for the basis of dietary miRNAs mediating cross-kingdom communication via food intake [68]. For example, miR166b-3p, miR159b-3p, miR159a and miR403-3p from broccoli-isolated EVs improved their survival compared to the naked (free) form [69].

In order to simulate the digestive environment more realistically, the digestive processes from the mouth (where the ERDNs are ingested in solid form) and the stomach (where the ERDNs are ingested in liquid form) were performed separately. The mean size of ERDNs did not change significantly during the continuous digestion of SGF+SIF. However, multiple peaks in the system obtained after SSF+SGF+SIF may be due to the addition of multiple enzymes. Salivary amylase was inactivated in an acidic environment and by pepsin hydrolysis. At the same time, pepsin was mainly active in a slightly acidic environment of pH = 2 to pH = 4, much less than in the digestive environment of the intestine (pH = 7) [42]. The stability of different sources of nanoparticles may vary. Grapefruit-derived nanoparticles show high tolerance to gastrointestinal enzymes and bile extracts, but the size of ginger-derived nanoparticles increased in SGF and further

increased in SIF [49,70]. Usually, the resistance of the carrier drug to the adverse conditions of digestion (oral, gastric and intestinal) is crucial for its therapeutic effect. The stability of PDEVs themselves during digestion favor their use as a nano drug delivery platform. This results showed that ERDNs could be used as drug carriers.

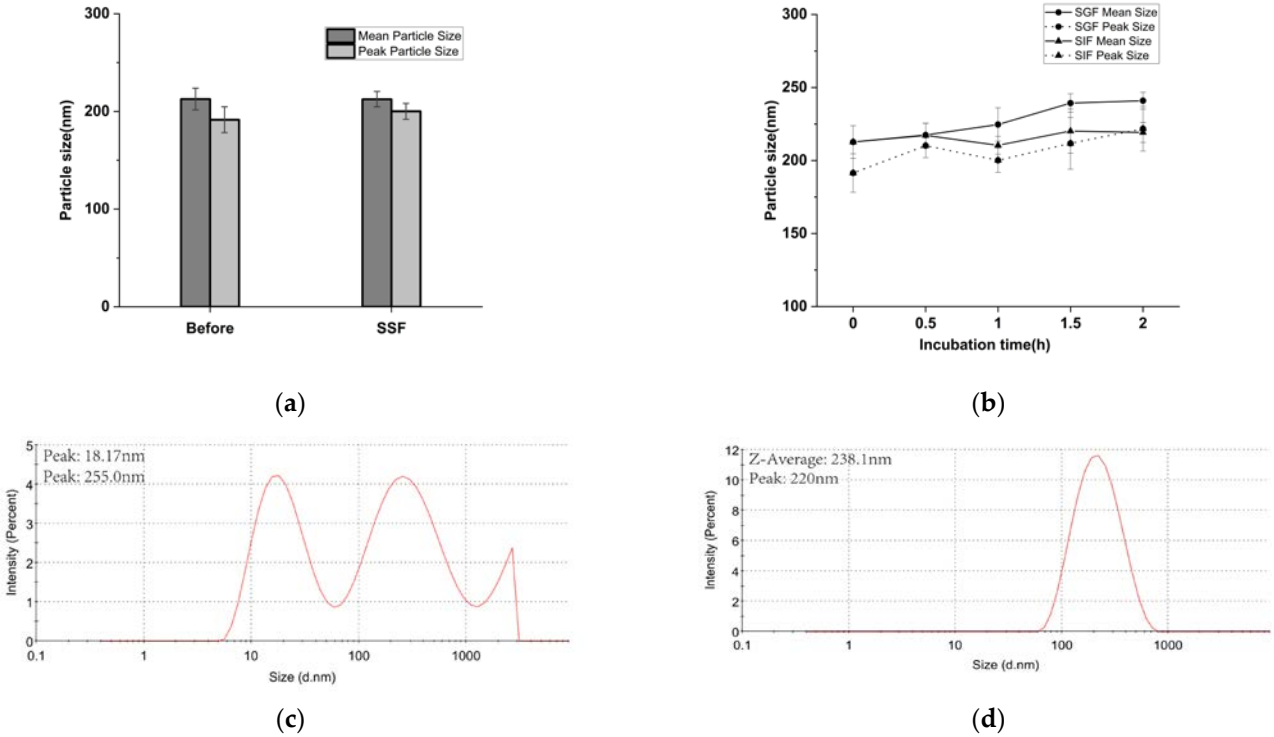

Figure 7. Particle size changes of ERDNs after vitro digestion simulation: (**a**) Particle size of ERDNs after 2 min of digestion in simulated salivary fluid (SSF). (**b**) Particle size changes of ERDNs at 2 h of digestion in simulated gastric fluid (SGF) and simulated intestinal fluid (SIF). (**c**) Particle distribution of ERDNs after continuous digestion in SSF, SGF and SIF by DLS. (**d**) Particle distribution of ERDNs after continuous digestion in SGF and SIF. The digestion times of the ERDNs in SSF, SGF and SIF were 2 min, 2 h and 2 h respectively.

4. Conclusions

In this study, ERDNs were successfully extracted from Raphani Semen. The PEG8000 method, using inexpensive and non-specialist equipment, gave higher yields than the conventional UC method, but was less specific and required other purification methods. For highly viscous substances, the use of sonication in the pre-treatment may assist in the dispersion of the system. The 8% PEG8000+SEC method extracted high-purity ERDNs and showed a range of proteins, suggesting that it could be used as a target for further downstream analysis. At the same time, the ERDNs were able to maintain stability during digestion in the stomach and intestine. Considering the similarity of exosome structures, this protocol could serve as a reference for the extraction and purification of other plant exosomes and provide ideas for the future development of functional foods with edible plant nanoparticles.

Author Contributions: In this study, Y.Z. contributed experimental ideas; J.A. conducted experimental operations and article writing. All authors have read and agreed to the published version of the manuscript.

Funding: This research received no external funding.

Data Availability Statement: The data generated and analyzed during this study are available from the corresponding author on necessary requests.

Acknowledgments: We would like to thank the Institute of Botany, Chinese Academy of Sciences for their support of the equipment and use of the ultracentrifuge in this experiment.

Conflicts of Interest: The authors declare no conflict of interest.

References

1. Al-Shehbaz, I.A.; Beilstein, M.; Kellogg, E. Systematics and phylogeny of the Brassicaceae (Cruciferae): An overview. *Plant Syst. Evol.* **2006**, *259*, 89–120. [CrossRef]
2. Ağagündüz, D.; Şahin, T.; Yılmaz, B.; Ekenci, K.D.; Özer, Ş.D.; Capasso, R. Cruciferous Vegetables and Their Bioactive Metabolites: From Prevention to Novel Therapies of Colorectal Cancer. *Evid. Based Complement. Altern. Med* **2022**, *2022*, 1534083. [CrossRef] [PubMed]
3. Melim, C.; Lauro, M.R.; Pires, I.M.; Oliveira, P.J.; Cabral, C. The Role of Glucosinolates from Cruciferous Vegetables (Brassicaceae) in Gastrointestinal Cancers: From Prevention to Therapeutics. *Pharmaceutics* **2022**, *14*, 190. [CrossRef] [PubMed]
4. Li, N.; Wu, X.; Zhuang, W.; Wu, C.; Rao, Z.; Du, L.; Zhou, Y. Cruciferous vegetable and isothiocyanate intake and multiple health outcomes. *Food Chem.* **2022**, *375*, 131816. [CrossRef]
5. Björkman, M.; Klingen, I.; Birch, A.N.; Bones, A.M.; Bruce, T.J.; Johansen, T.J.; Meadow, R.; Mølmann, J.; Seljåsen, R.; Smart, L.E.; et al. Phytochemicals of Brassicaceae in plant protection and human health—Influences of climate, environment and agronomic practice. *Phytochemistry* **2011**, *72*, 538–556. [CrossRef]
6. Poddar, K.H.; Sikand, G.; Kalra, D.; Wong, N.; Duell, P.B. Mustard oil and cardiovascular health: Why the controversy? *J. Clin. Lipidol.* **2022**, *16*, 13–22. [CrossRef]
7. Chinese Pharmacopoeia Commission. *Pharmacopoeia of the People's Republic of China*; China Medical Science Publisher: Beijing, China, 2020.
8. Gao, L.; Li, H.; Li, B.; Shao, H.; Yu, X.; Miao, Z.; Zhang, L.; Zhu, L.; Sheng, H. Traditional uses, phytochemistry, transformation of ingredients and pharmacology of the dried seeds of *Raphanus sativus* L. (Raphani Semen): A comprehensive review. *J. Ethnopharmacol.* **2022**, *294*, 115387. [CrossRef]
9. Kim, K.H.; Kim, C.S.; Park, Y.J.; Moon, E.; Choi, S.U.; Lee, J.H.; Kim, S.Y.; Lee, K.R. Anti-inflammatory and antitumor phenylpropanoid sucrosides from the seeds of Raphanus sativus. *Bioorg. Med. Chem. Lett.* **2015**, *25*, 96–99. [CrossRef]
10. Kim, K.H.; Moon, E.; Lee, S.R.; Park, K.J.; Kim, S.Y.; Choi, S.U.; Lee, K.R. Chemical Constituents of the Seeds of *Raphanus sativus* and their Biological Activity. *J. Braz. Chem. Soc.* **2015**, *26*, 2307–2312.
11. Choi, K.-C.; Cho, S.-W.; Kook, S.-H.; Chun, S.-R.; Bhattarai, G.; Poudel, S.B.; Kim, M.-K.; Lee, K.-Y.; Lee, J.-C. Intestinal anti-inflammatory activity of the seeds of *Raphanus sativus* L. in experimental ulcerative colitis models. *J. Ethnopharmacol.* **2016**, *179*, 55–65. [CrossRef]
12. Park, W.Y.; Song, G.; Noh, J.H.; Kim, T.; Kim, J.J.; Hong, S.; Park, J.; Um, J.-Y. Raphani Semen (*Raphanus sativus* L.) Ameliorates Alcoholic Fatty Liver Disease by Regulating De Novo Lipogenesis. *Nutrients* **2021**, *13*, 448. [CrossRef] [PubMed]
13. Qian, B.; Pan, Y.; Cai, Z.; Jing, P. Phytochemical composition, antioxidant capacity and ACE-inhibitory activity of China-grown radish seeds. *J. Appl. Bot. Food Qual.* **2017**, *90*, 315–322.
14. Gao, S.; Wang, J.; Cheng, L.; Fan, Y.; Qin, W.; Wang, Y.; Guo, Y.; Zhang, X.; Yang, Y. Evaluation of the Effects of Processing Technique on Chemical Components in Raphani Semen by HPLC and UPLC-Q-TOF-MS. *Int. J. Anal. Chem.* **2022**, *2022*, 8279839. [CrossRef] [PubMed]
15. Pan, B.T.; Johnstone, R.M. Fate of the transferrin receptor during maturation of sheep reticulocytes in vitro: Selective externalization of the receptor. *Cell* **1983**, *33*, 967–978. [CrossRef] [PubMed]
16. Halperin, W.; Jensen, W.A. Ultrastructural changes during growth and embryogenesis in carrot cell cultures. *J. Ultrastruct. Res.* **1967**, *18*, 428–443. [CrossRef]
17. Man, F.; Wang, J.; Lu, R. Techniques and Applications of Animal- and Plant-Derived Exosome-Based Drug Delivery System. *J. Biomed. Nanotechnol.* **2020**, *16*, 1543–1569. [CrossRef]
18. Kalluri, R.; LeBleu, V.S. The biology, function, and biomedical applications of exosomes. *Science* **2020**, *367*, eaau6977. [CrossRef]
19. Sfragano, P.S.; Pillozzi, S.; Condorelli, G.; Palchetti, I. Practical tips and new trends in electrochemical biosensing of cancer-related extracellular vesicles. *Anal. Bioanal. Chem.* **2023**, *415*, 1087–1106. [CrossRef]
20. Sadeghi, S.; Tehrani, F.R.; Tahmasebi, S.; Shafiee, A.; Hashemi, S.M. Exosome engineering in cell therapy and drug delivery. *Inflammopharmacology* **2023**, *31*, 145–169. [CrossRef]
21. Yang, C.; Zhang, M.; Merlin, D. Advances in Plant-derived Edible Nanoparticle-based lipid Nano-drug Delivery Systems as Therapeutic Nanomedicines. *J. Mater. Chem. B* **2018**, *6*, 1312–1321. [CrossRef]
22. Mu, J.; Zhuang, X.; Wang, Q.; Jiang, H.; Deng, Z.B.; Wang, B.; Zhang, L.; Kakar, S.; Jun, Y.; Miller, D.; et al. Interspecies communication between plant and mouse gut host cells through edible plant derived exosome-like nanoparticles. *Mol. Nutr. Food Res.* **2014**, *58*, 1561–1573. [CrossRef] [PubMed]
23. Baldini, N.; Torreggiani, E.; Roncuzzi, L.; Perut, F.; Zini, N.; Avnet, S. Exosome-like Nanovesicles Isolated from *Citrus limon* L. Exert Antioxidative Effect. *Curr. Pharm. Biotechnol.* **2018**, *19*, 877–885. [CrossRef] [PubMed]

24. Deng, Z.; Rong, Y.; Teng, Y.; Mu, J.; Zhuang, X.; Tseng, M.; Samykutty, A.; Zhang, L.; Yan, J.; Miller, D.; et al. Broccoli-Derived Nanoparticle Inhibits Mouse Colitis by Activating Dendritic Cell AMP-Activated Protein Kinase. *Mol. Ther.* **2017**, *25*, 1641–1654. [CrossRef] [PubMed]
25. Liu, B.; Lu, Y.; Chen, X.; Muthuraj, P.G.; Li, X.; Pattabiraman, M.; Zempleni, J.; Kachman, S.D.; Natarajan, S.K.; Yu, J. Protective Role of Shiitake Mushroom-Derived Exosome-Like Nanoparticles in D-Galactosamine and Lipopolysaccharide-Induced Acute Liver Injury in Mice. *Nutrients* **2020**, *12*, 477. [CrossRef]
26. Zhang, L.; Hou, D.; Chen, X.; Li, D.; Zhu, L.; Zhang, Y.; Li, J.; Bian, Z.; Liang, X.; Cai, X.; et al. Exogenous plant MIR168a specifically targets mammalian LDLRAP1: Evidence of cross-kingdom regulation by microRNA. *Cell Res.* **2012**, *22*, 107–126. [CrossRef]
27. Zhang, M.; Viennois, E.; Prasad, M.; Zhang, Y.; Wang, L.; Zhang, Z.; Han, M.K.; Xiao, B.; Xu, C.; Srinivasan, S.; et al. Edible ginger-derived nanoparticles: A novel therapeutic approach for the prevention and treatment of inflammatory bowel disease and colitis-associated cancer. *Biomaterials* **2016**, *101*, 321–340. [CrossRef]
28. Teng, Y.; Ren, Y.; Sayed, M.; Hu, X.; Lei, C.; Kumar, A.; Hutchins, E.; Mu, J.; Deng, Z.; Luo, C.; et al. Plant-Derived Exosomal MicroRNAs Shape the Gut Microbiota. *Cell Host Microbe* **2018**, *24*, 637–652.e8. [CrossRef]
29. Théry, C.; Witwer, K.W.; Aikawa, E.; Alcaraz, M.J.; Anderson, J.D.; Andriantsitohaina, R.; Antoniou, A.; Arab, T.; Archer, F.; Atkin-Smith, G.K.; et al. Minimal information for studies of extracellular vesicles 2018 (MISEV2018): A position statement of the International Society for Extracellular Vesicles and update of the MISEV2014 guidelines. *J. Extracell. Vesicles.* **2018**, *7*, 1535750. [CrossRef]
30. Li, K.; Wong, D.K.; Hong, K.Y.; Raffai, R.L. Cushioned-Density Gradient Ultracentrifugation (C-DGUC): A Refined and High Performance Method for the Isolation, Characterization, and Use of Exosomes. *Methods Mol. Biol.* **2018**, *1740*, 69–83.
31. Zeringer, E.; Barta, T.; Li, M.; Vlassov, A.V. Strategies for isolation of exosomes. *Cold Spring Harb. Protoc.* **2015**, *2015*, 319–323. [CrossRef]
32. Linares, R.; Tan, S.; Gounou, C.; Arraud, N.; Brisson, A.R. High-speed centrifugation induces aggregation of extracellular vesicles. *J. Extracell. Vesicles* **2015**, *4*, 29509. [CrossRef] [PubMed]
33. Kalarikkal, S.P.; Prasad, D.; Kasiappan, R.; Chaudhari, S.R.; Sundaram, G.M. A cost-effective polyethylene glycol-based method for the isolation of functional edible nanoparticles from ginger rhizomes. *Sci. Rep.* **2020**, *10*, 4456. [CrossRef] [PubMed]
34. Zhou, Y.; McNamara, R.; Dittmer, D. Purification Methods and the Presence of RNA in Virus Particles and Extracellular Vesicles. *Viruses* **2020**, *12*, 917. [CrossRef] [PubMed]
35. Deregibus, M.C.; Figliolini, F.; D'Antico, S.; Manzini, P.M.; Pasquino, C.; De Lena, M.; Tetta, C.; Brizzi, M.F.; Camussi, G. Charge-based precipitation of extracellular vesicles. *Int. J. Mol. Med.* **2016**, *38*, 1359–1366. [CrossRef] [PubMed]
36. You, J.Y.; Kang, S.J.; Rhee, W.J. Isolation of cabbage exosome-like nanovesicles and investigation of their biological activities in human cells. *Bioact. Mater.* **2021**, *6*, 4321–4332. [CrossRef] [PubMed]
37. Regente, M.; Corti-Monzón, G.; Maldonado, A.M.; Pinedo, M.; Jorrín, J.; de la Canal, L. Vesicular fractions of sunflower apoplastic fluids are associated with potential exosome marker proteins. *FEBS Lett.* **2009**, *583*, 3363–3366. [CrossRef] [PubMed]
38. Xu, F.; Mu, J.; Teng, Y.; Zhang, X.; Sundaram, K.; Sriwastva, M.K.; Kumar, A.; Lei, C.; Zhang, L.; Liu, Q.M.; et al. Restoring Oat Nanoparticles Mediated Brain Memory Function of Mice Fed Alcohol by Sorting Inflammatory Dectin-1 Complex Into Microglial Exosomes. *Small* **2022**, *18*, e2105385. [CrossRef]
39. Peters, D.L.; Harris, G.; Davis, C.M.; Dennis, J.J.; Chen, W. Bacteriophage Isolation, Purification, and Characterization Techniques Against Ubiquitous Opportunistic Pathogens. *Curr. Protoc.* **2022**, *2*, e594. [CrossRef]
40. Dumke, R.; Geissler, M.; Skupin, A.; Helm, B.; Mayer, R.; Schubert, S.; Oertel, R.; Renner, B.; Dalpke, A. Simultaneous Detection of SARS-CoV-2 and Influenza Virus in Wastewater of Two Cities in Southeastern Germany, January to May 2022. *Int. J. Environ. Res. Public Health* **2022**, *19*, 13374. [CrossRef]
41. Pandey, M.; Chawla, G. Purification of exosome-enriched proteins produced in a Drosophila cell line by size exclusion chromatography. *STAR Protoc.* **2022**, *3*, 101834. [CrossRef]
42. Minekus, M.; Alminger, M.; Alvito, P.; Ballance, S.; Bohn, T.; Bourlieu, C.; Carrière, F.; Boutrou, R.; Corredig, M.; Dupont, D.; et al. A standardised static in vitro digestion method suitable for food—An international consensus. *Food Funct.* **2014**, *5*, 1113–1124. [CrossRef] [PubMed]
43. Alić, V.K.; Malenica, M.; Biberić, M.; Zrna, S.; Valenčić, L.; Šuput, A.; Fabris, L.K.; Wechtersbach, K.; Kojc, N.; Kurtjak, M.; et al. Extracellular Vesicles from Human Cerebrospinal Fluid Are Effectively Separated by Sepharose CL-6B-Comparison of Four Gravity-Flow Size Exclusion Chromatography Methods. *Biomedicines* **2022**, *10*, 785. [CrossRef] [PubMed]
44. An, M.; Wu, J.; Zhu, J.; Lubman, D.M. Comparison of an Optimized Ultracentrifugation Method versus Size-Exclusion Chromatography for Isolation of Exosomes from Human Serum. *J. Proteome Res.* **2018**, *17*, 3599–3605. [CrossRef] [PubMed]
45. Wang, Y.; Wang, J.; Ma, J.; Zhou, Y.; Lu, R. Focusing on Future Applications and Current Challenges of Plant Derived Extracellular Vesicles. *Pharmaceuticals* **2022**, *15*, 708. [CrossRef]
46. Ju, S.; Mu, J.; Dokland, T.; Zhuang, X.; Wang, Q.; Jiang, H.; Xiang, X.; Deng, Z.-B.; Wang, B.; Zhang, L.; et al. Grape exosome-like nanoparticles induce intestinal stem cells and protect mice from DSS-induced colitis. *Mol. Ther.* **2013**, *21*, 1345–1357. [CrossRef]
47. Rome, S. Biological properties of plant-derived extracellular vesicles. *Food Funct.* **2019**, *10*, 529–538. [CrossRef]
48. Yang, M.; Luo, Q.; Chen, X.; Chen, F. Bitter melon derived extracellular vesicles enhance the therapeutic effects and reduce the drug resistance of 5-fluorouracil on oral squamous cell carcinoma. *J. Nanobiotechnol.* **2021**, *19*, 259. [CrossRef]

49. Wang, B.; Zhuang, X.; Deng, Z.-B.; Jiang, H.; Mu, J.; Wang, Q.; Xiang, X.; Guo, H.; Zhang, L.; Dryden, G.; et al. Targeted drug delivery to intestinal macrophages by bioactive nanovesicles released from grapefruit. *Mol. Ther.* **2014**, *22*, 522–534. [CrossRef]
50. Kim, J.; Li, S.; Zhang, S.; Wang, J. Plant-derived exosome-like nanoparticles and their therapeutic activities. *Asian J. Pharm. Sci.* **2022**, *17*, 53–69. [CrossRef]
51. Zu, M.; Xie, D.; Canup, B.S.; Chen, N.; Wang, Y.; Sun, R.; Zhang, Z.; Fu, Y.; Dai, F.; Xiao, B. 'Green' nanotherapeutics from tea leaves for orally targeted prevention and alleviation of colon diseases. *Biomaterials* **2021**, *279*, 121178. [CrossRef]
52. Ludwig, A.-K.; De Miroschedji, K.; Doeppner, T.R.; Börger, V.; Ruesing, J.; Rebmann, V.; Durst, S.; Jansen, S.; Bremer, M.; Behrmann, E.; et al. Precipitation with polyethylene glycol followed by washing and pelleting by ultracentrifugation enriches extracellular vesicles from tissue culture supernatants in small and large scales. *J. Extracell. Vesicles* **2018**, *7*, 1528109. [CrossRef]
53. Weng, Y.; Sui, Z.; Shan, Y.; Hu, Y.; Chen, Y.; Zhang, L.; Zhang, Y. Effective isolation of exosomes with polyethylene glycol from cell culture supernatant for in-depth proteome profiling. *Analyst* **2016**, *141*, 4640–4646. [CrossRef] [PubMed]
54. Matrajt, G.; Naughton, B.; Bandyopadhyay, A.S.; Meschke, J.S. A Review of the Most Commonly Used Methods for Sample Collection in Environmental Surveillance of Poliovirus. *Clin. Infect. Dis.* **2018**, *67* (Suppl. S1), S90–S97. [CrossRef]
55. Cong, M.; Tan, S.; Li, S.; Gao, L.; Huang, L.; Zhang, H.G.; Qiao, H. Technology insight: Plant-derived vesicles-How far from the clinical biotherapeutics and therapeutic drug carriers? *Adv. Drug Deliv. Rev.* **2022**, *182*, 114108. [CrossRef] [PubMed]
56. D'Souza, A.A.; Shegokar, R. Polyethylene glycol (PEG): A versatile polymer for pharmaceutical applications. *Expert Opin. Drug Deliv.* **2016**, *13*, 1257–1275. [CrossRef] [PubMed]
57. Yamamoto, K.R.; Alberts, B.M.; Benzinger, R.; Lawhorne, L.; Treiber, G. Rapid bacteriophage sedimentation in the presence of polyethylene glycol and its application to large-scale virus purification. *Virology* **1970**, *40*, 734–744. [CrossRef] [PubMed]
58. Gould, S.J.; Booth, A.M.; Hildreth, J.E.K. The Trojan exosome hypothesis. *Proc. Natl. Acad. Sci. USA* **2003**, *100*, 10592–10597. [CrossRef] [PubMed]
59. Rider, M.A.; Hurwitz, S.N.; Meckes, D.G., Jr. ExtraPEG: A Polyethylene Glycol-Based Method for Enrichment of Extracellular Vesicles. *Sci. Rep.* **2016**, *6*, 23978. [CrossRef] [PubMed]
60. Madera-Contreras, A.M.; Solano-Texta, R.; Cisneros-Sarabia, A.; Bautista-Santos, I.; Vences-Velázquez, G.; Vences-Velázquez, A.; Cortés-Sarabia, K. Optimized method for the extraction of contaminant-free IgY antibodies from egg yolk using PEG 6000. *MethodsX* **2022**, *9*, 101874. [CrossRef]
61. Sunoqrot, S.; Al-Bakri, A.G.; Ibrahim, L.H.; Aldaken, N. Amphotericin B-Loaded Plant-Inspired Polyphenol Nanoparticles Enhance Its Antifungal Activity and Biocompatibility. *ACS Appl. Bio. Mater.* **2022**, *5*, 5156–5164. [CrossRef]
62. Carroll-Portillo, A.; Coffman, C.; Varga, M.; Alcock, J.; Singh, S.; Lin, H. Standard Bacteriophage Purification Procedures Cause Loss in Numbers and Activity. *Viruses* **2021**, *13*, 328. [CrossRef] [PubMed]
63. Yun, L.; Wu, T.; Mao, Z.; Li, W.; Zhang, M.; Sun, X. A novel wheat germ polysaccharide: Structural characterization, potential antioxidant activities and mechanism. *Int. J. Biol. Macromol.* **2020**, *165 Pt B*, 1978–1987. [CrossRef]
64. Shao, K.; Sun, J.; Lin, Y.; Zhi, H.; Wang, X.; Fu, Y.; Xu, J.; Liu, Z. Green Synthesis and Antimicrobial Study on Functionalized Chestnut-Shell-Extract Ag Nanoparticles. *Antibiotics* **2023**, *12*, 201. [CrossRef] [PubMed]
65. Cassari, L.; Zamuner, A.; Messina, G.M.L.; Marsotto, M.; Chen, H.; Gonnella, G.; Coward, T.; Battocchio, C.; Huang, J.; Iucci, G.; et al. Bioactive PEEK: Surface Enrichment of Vitronectin-Derived Adhesive Peptides. *Biomolecules* **2023**, *13*, 246. [CrossRef] [PubMed]
66. Suresh, A.P.; Kalarikkal, S.P.; Pullareddy, B.; Sundaram, G.M. Low pH-Based Method to Increase the Yield of Plant-Derived Nanoparticles from Fresh Ginger Rhizomes. *ACS Omega* **2021**, *6*, 17635–17641. [CrossRef]
67. Samak, Y.O.; Santhanes, D.; El-Massik, M.A.; Coombes, A.G.A. Formulation strategies for achieving high delivery efficiency of thymoquinone-containing Nigella sativa extract to the colon based on oral alginate microcapsules for treatment of inflammatory bowel disease. *J. Microencapsul.* **2019**, *36*, 204–214. [CrossRef]
68. Qin, X.; Wang, X.; Xu, K.; Zhang, Y.; Ren, X.; Qi, B.; Liang, Q.; Yang, X.; Li, L.; Li, S. Digestion of Plant Dietary miRNAs Starts in the Mouth under the Protection of Coingested Food Components and Plant-Derived Exosome-like Nanoparticles. *J. Agric. Food Chem.* **2022**, *70*, 4316–4327. [CrossRef]
69. del Pozo-Acebo, L.; de Las Hazas, M.C.; Tomé-Carneiro, J.; del Saz-Lara, A.; Gil-Zamorano, J.; Balaguer, L.; Chapado, L.A.; Busto, R.; Visioli, F.; Dávalos, A. Therapeutic potential of broccoli-derived extracellular vesicles as nanocarriers of exogenous miRNAs. *Pharmacol. Res.* **2022**, *185*, 106472. [CrossRef]
70. Li, Z.; Wang, H.; Yin, H.; Bennett, C.; Zhang, H.; Guo, P. Ginger-derived nanoparticles protect against alcohol-induced liver damage. *J. Extracell. Vesicles* **2015**, *4*, 28713.